Biofouling, October 2003 Vol 19 (5), pp 279–285

Taylor & Francis
Taylor & Francis Group

Viscoelastic Properties of a Mixed Culture Biofilm from Rheometer Creep Analysis

BRETT W TOWLER[a], CORY J RUPP[b,c], AL B CUNNINGHAM[a,c] and PAUL STOODLEY[a,c,d,*]

[a]*Department of Civil Engineering, Montana State University, Bozeman 59717, USA;* [b]*Department of Mechanical Engineering, Montana State University, Bozeman 59717, USA;* [c]*Center for Biofilm Engineering, Montana State University, Bozeman 59717, USA;* [d]*Department of Microbiology, Montana State University, Bozeman 59717, USA*

(Received 25 March 2003; in final form 15 May 2003)

The mechanical properties of mixed culture biofilms were determined by creep analysis using an AR1000 rotating disk rheometer. The biofilms were grown directly on the rheometer disks which were rotated in a chemostat for 12 d. The resulting biofilms were heterogeneous and ranged from 35 μm to 50 μm in thickness. The creep curves were all viscoelastic in nature. The close agreement between stress and strain ratio of a sample tested at 0.1 and 0.5 Pa suggested that the biofilms were tested in the linear viscoelastic range and supported the use of linear viscoelastic theory in the development of a constitutive law. The experimental data was fit to a 4-element Burger spring and dashpot model. The shear modulus (G) ranged from 0.2 to 24 Pa and the viscous coefficient (η) from 10 to 3000 Pa. These values were in the same range as those previously estimated from fluid shear deformation of biofilms in flow cells. A viscoelastic biofilm model will help to predict shear related biofilm phenomena such as elevated pressure drop, detachment, and the flow of biofilms over solid surfaces.

Keywords: biofilm; Burger model; creep; mechanical properties; rheometry; viscoelasticity

INTRODUCTION

As materials, biofilms are complex composites consisting of microbial cells, extruded polysaccharides, proteins, nucleic acids, and possibly sediments and precipitates. The complex mechanical nature of biofilms may contribute to many unique engineering problems. Biofilm accumulation can cause significant pressure loss in water distribution systems and piping networks (Characklis, 1973; Zelver, 1979; Picaloglou *et al*., 1980). Furthermore, this bacterial growth can result in increased hydrodynamic drag on ship hulls and, consequently, increased fuel consumption (Cooksey & Wigglesworth-Cooksey, 1995; Schultz & Swain, 2000; Townsin, 2003). It has been postulated that this energy loss is influenced by the highly compliant nature of a biofilm (Picaloglou *et al*., 1980; Stoodley *et al*., 1999a). The mechanical properties of biofilms will also determine when and how a biofilm fails and detaches in response to a physical force such as fluid-induced shear. Detachment is a serious concern in the management of drinking water supply systems as detached biofilms can contribute to contamination and the distribution of pathogens (Walker *et al*., 1995). Prevention of this phenomenon is also important in the field of medicine. For example, the growth of biofilm on medical devices can result in persistent infections (Costerton *et al*., 1999) and the detachment of dental biofilms associated with periodontal disease has been linked to a range of systemic diseases (Newman, 1998).

In flowing systems, the processes of biofilm deformation and failure are largely influenced by the stresses applied by a moving fluid and the material properties of the bacterial biofilm. Previous work has suggested that laboratory-grown biofilms are viscoelastic in nature (Stoodley *et al*., 1999a; Fleming *et al*., 2000; Koerstgens *et al*., 2001; Klapper *et al*., 2002). The properties calculated by Stoodley *et al*. (1999a) were based on the induced strain of individual biofilm microcolonies growing in glass tube flow cells by varying the fluid shear of biofilm in which the three-dimensional deformation was approximated as a one-dimensional uniaxial strain. Although the uniaxial elongation could be measured quite precisely by microscopy, the shear stress acting on individual microcolonies could only be approximated as the theoretical

*Corresponding author; e-mail: paul_s@erc.montana.edu

ISSN 0892-7014 print/ISSN 1029-2454 online
DOI: 10.1080/0892701031000152470

shear in clean tubes (Stoodley *at al.*, 1999a). Since the shear was varied by manually changing the pump speed, high frequency dynamic testing was not possible so the creep response to shear was measured. To build on these data the creep response of mixed culture biofilms was investigated using spinning disk rheometery, a well-established technique for measuring viscoelastic properties in which shear stress and strain are precisely monitored (Findley *et al.*, 1989). Parallel plates were used for testing since flat surfaces have the advantage for biofilm studies that they are more readily incorporated into growth reactors and are conducive for growing uniformly distributed biofilms. They have the additional advantage over cone and plate and concentric ring geometries in that i) the gap thickness between surfaces is uniform and ii) the gap can be easily adjusted to accommodate biofilms of different thickness. Also, biofilm samples can be grown directly on the rheometer disks under a rotational fluid shear stress (τ) so that the growth conditions are similar to the testing conditions. The main disadvantage is that the shear rate is not constant across the radius. Relating material properties back to applied torque involves solving a derivative of torque with respect to velocity gradient. Historically, this was problematic. However, instruments operated by computer overcome this limitation by calculating this derivative by first numerically converting discrete data points into a continuous function using cubic splines. Shear creep tests on the biofilms allowed a one-dimensional shear-strain (γ) analysis based on a standard mechanical testing procedure. The creep curves were modelled with a system of springs and dashpots from which a constitutive equation, which relates strain (physical deformation) to mechanical stress (Flugge, 1975; Mase & Mase, 1999), was derived. Expressing the relationship between mechanical forces and biofilm deformation in a constitutive law is an important step in modelling, predicting, and ultimately controlling, phenomena directly related to biofilm mechanics such as detachment, pressure drop, and biofilm stability.

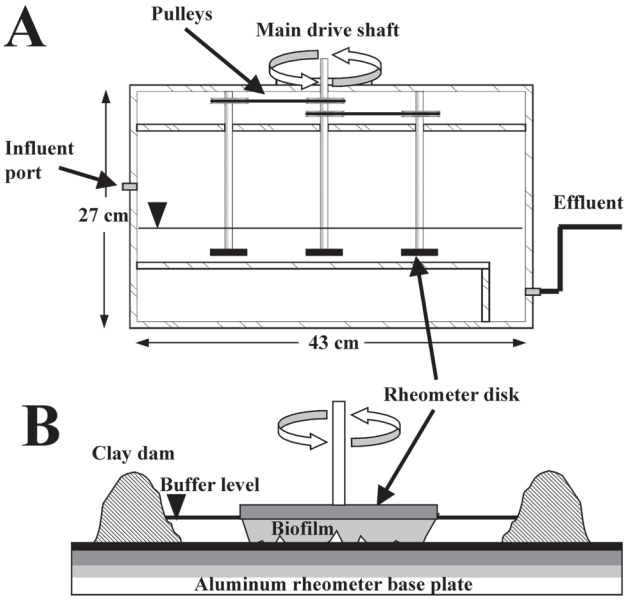

FIGURE 1 A) Biofilm growth chamber, drive shafts, pulleys and rheometer disks. B) Orientation of rheometer disk and biofilm when placed in the AR1000 for creep testing.

MATERIALS AND METHODS

Biofilm Growth Reactor

The biofilm growth reactor consisted of a polycarbonate growth chamber (Figure 1A), a 1 amp electric motor, a peristaltic pump and two 5 gallon glass carboys. The top cover of the growth chamber was removable and contained a sealed bearing through which the drive shaft was held. A bridge assembly, which housed two secondary drive pulleys, was anchored to the bottom of this top cover. The main drive shaft was connected to the electric motor and rotated the secondary shafts through the pulley system. A 40 mm diameter anodized aluminum rheometer parallel disk 'geometry' was secured to the end of each of the three drive shafts. These disks were positioned 5 mm above the chamber floor. The depth of the water above the growth surface was approximately 5 mm. The angular velocity of the shaft/disk was held constant at 20 rpm throughout the experiments. At this rpm the angular velocity at the outside edge of the disk was 4.2 cm s^{-1} and the corresponding Reynolds (Re) number was 208 (taking the distance between the disk surface and the bottom of the reactor (0.5 cm) as the characteristic distance). Since the Re indicated that flow was laminar a linear velocity gradient was assumed between the no-slip condition at the surface of the disk and the bottom of the reactor. The shear stress was found from the product of the velocity gradient and the viscosity of the aqueous medium (assumed to be equal to that of water). From these calculations it was estimated that the shear stress varied linearly from 0 mPa at the center of the disk to 8.4 mPa at the edge. Four independent replicate experiments containing triplicate samples were conducted.

Nutrients

Luria-Bertani broth ($^1/_{100}$ strength LB, 2 g l^{-1}) was used to grow the biofilms. Nutrients were pumped into the growth chamber at a constant flow rate of 2.0 ml min^{-1}, which resulted in a hydraulic residence time (θ_H) of 7.8 h. Gravity discharge from an

effluent port maintained the nutrient depth at a constant level.

Inoculation

The chamber was inoculated with a 5 ml sample of water from the Montana State University duck pond. The inoculum was injected into the reactor through a sealed port tapped into the front face of the chamber. The system was operated as a batch culture for the first 24 h period (day 1), to allow for the attachment of cells to the disks. From day 2 the influent was turned on and the system operated as a continuous culture. In order to limit algal growth, the entire growth chamber was covered with cardboard sheeting.

Rheometry

Samples were removed from the growth chamber on day 12 for testing on a TA Instruments AR1000 Rheometer (www.tainst.com). Disks were removed from the drives shafts and placed in Ringers salts for transport to the material-testing laboratory. The disks, with attached biofilms, were installed into the rheometer using a gap setting of 30 μm. This gap was based on measurements of biofilm thickness made with an epi-fluorescent microscope. The disks were oriented such that the direction of rotation of the disk during growth and the direction of the applied stress for the creep test were consistent. To prevent de-watering of the sample during testing, the tests were performed in submersion by fashioning a water dam around the edges of the instrument's base-plate, using modelling clay (Figure 1B). Shear creep tests were performed by applying a constant shear stress (τ) and measuring shear strain (γ) over time. During the development of the methods for these tests, several different τ values were examined. It was observed that τ in excess of 1.0 Pa frequently resulted in a strain response that closely approximated a Newtonian fluid (data not shown), suggesting that a τ of 1.0 Pa was beyond the yield point of the biofilm. Biofilm was still visibly attached after inspection of the disk suggesting that yielding was due to cohesive, rather than adhesive, failure. Based on these results standard tests were conducted by applying a τ of 0.1 Pa (measured at the at the edge of the rheometer plate) for a 3 min retardation (loading) period, followed by a 3 min recovery (unloading) period ($\tau = 0$). Approximately 900 measurements of strain *vs* time were taken over each 6 min test. To determine if the material behaved in a linear viscoelastic manner (in this context where γ is proportional to τ) at this test shear, one sample was tested again after a recovery period of 7 min with a τ of 0.5 Pa. A total of 10 biofilms were tested from either 2 or 3 plates from each of 4 independent experiments.

Modelling

The creep curves were modelled using a system of springs (elastic elements) and dashpots (viscous elements). Since the step between the retardation and recovery periods of the creep tests prevented the use of any derivative based non-linear regression technique, an iterative algorithm was used to determine the optimized material parameters in the model. The algorithm involved four steps, *viz*. i) the domain of each of the material parameters was discretized over an estimated range, ii) the strain response was calculated for each of these combinations of parameters over the entire time domain, iii) the combination that produced the lowest error in predicting the experimental data was identified using a residual function. The following residual function was weighted by the size of the time step and was regarded as the difference in areas under the observed and predicted creep curves.

$$WR = \frac{1}{\sum_{i=0}^{N} dt_i}\left[\int_{t=t^0}^{t=tN} \gamma_P(t)dt - \sum_{i=0}^{N} \gamma_o^i dt^i\right] \qquad [1]$$

where dt is the time step (s), γ_P is the predicted strain, and γ_0 is the observed strain for $i = 1$ to N data points. The non-dimensional weighted residuals (NWR) (ratios of the weighted residuals to the maximum observed strains) were used to gauge the accuracy of the model. By normalizing the WR against the maximum strain for each data set, a universal measure of accuracy was achieved. iv) If the NWR was < 0.05, the identified combination of material coefficients was selected as the optimized fit. If not, the sizes of the parameter domains were reduced, re-centered on the combination with the lowest error, and the process was repeated. Using this procedure, the experimental data were fitted to several different linear viscoelastic constitutive equations (MathWorks Incorporated MATLAB 6.1). Eight data sets were chosen for modelling purposes.

RESULTS

Biofilms

After 12 d heterogeneous biofilms had grown on each of the rheometer geometries (Figure 2). The thickness of the biofilm varied from approximately 35 μm to 50 μm. Although heterogeneous at the micro-scale, macroscopic observation showed that coverage of the

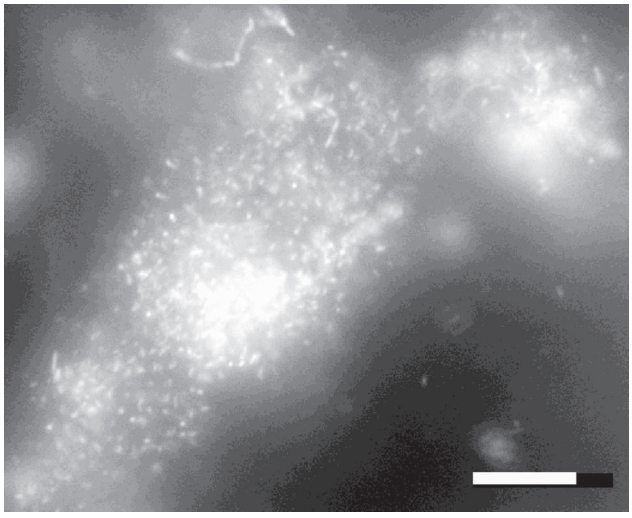

FIGURE 2 Epifluorescent image of the top of the mixed species biofilm grown on a rheometer disk showing bacterial rods, cocci, and chains. Scale bar = 20 μm.

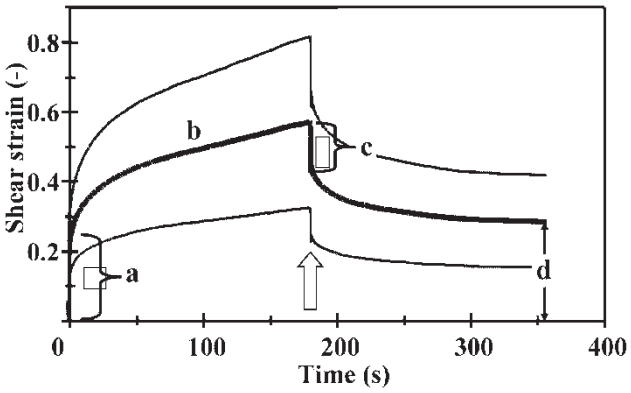

FIGURE 3 Mean shear strain (thick line) from 10 creep curves of separate biofilms demonstrate a classic viscoelastic response. The applied τ of 0.1 Pa was removed after 180 s (arrow). The flanking thinner lines are $\pm$ 1 SE. The curve can be divided into various components, *viz*. a) instantaneous elastic response (I_γ), b) time dependent viscous response, c) instantaneous elastic recovery after τ was removed, and d) unrecoverable viscous strain (V_γ).

rheometer disk was relatively uniform and 10 of the 12 samples that had biofilm covering the entire surface were selected for creep tests.

Creep Tests

The character of the strain responses for all 10 biofilms tested at 0.1 Pa was clearly viscoelastic in nature (Figure 3). Each curve exhibited an instantaneous elastic response (I_γ) and recovery, a time-dependent viscous deformation, and an unrecoverable viscous loss (V_γ).

Linearity

To assess the linearity of the strain responses the two data sets for sample 3 (τ = 0.1 and τ = 0.5) were plotted (Figure 4) and a least-squares linear regression was made. The regression produced a proportionality constant, *c*, of 5.0843 (R^2 of 0.8819), which was almost exactly the proportional increase in the shear stress.

Constitutive Equations

All of the creep curves indicated the existence of instantaneous, time-dependent, and viscous responses. The 4-element Burger model (Figure 5) is the simplest analogue that can approximate all three of these responses (Findley *et al.*, 1989). The constitutive law in differential equation form for the Burger model is:

$$\tau + \left(\frac{\eta_1}{G_1} + \frac{\eta_1}{G_2} + \frac{\eta_2}{G_2}\right)\frac{\partial \tau}{\partial t} + \left(\frac{\eta_1\eta_2}{G_1G_2}\right)\frac{\partial^2 \tau}{\partial t^2} = \eta_1\frac{\partial \gamma}{\partial t} + \left(\frac{\eta_1\eta_2}{G_2}\right)\frac{\partial^2 \gamma}{\partial t^2} \qquad [2]$$

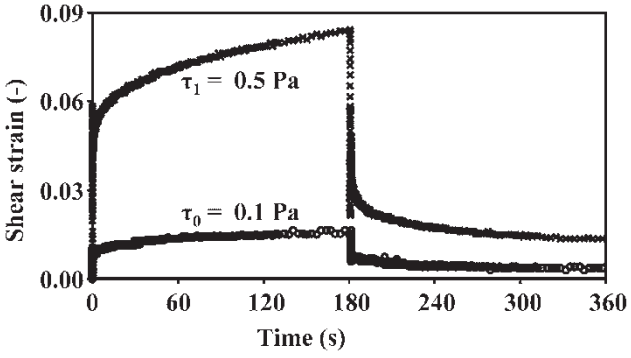

FIGURE 4 Creep curves run at τ = 0.1 and 0.5 Pa on the same biofilm to determine if the biofilm was being tested within the linear viscoelastic region. The fivefold increase in τ resulted in a fivefold increase in strain demonstrating linearity.

And its shear creep strain response is

$$\gamma(t) = \tau_o\left[\frac{1}{G_1} + \frac{t}{\eta_1} + \frac{1}{G_2}\left(1 - e^{-G_2 t/\eta_2}\right)\right] \qquad [3a]$$

$$\gamma(t) = \tau_o\left[\frac{t_s}{\eta_1} + \frac{1}{G_2}\left(e^{-G_2 t_s/\eta_2} - 1\right)e^{-G_2 t/\eta_2}\right] \qquad [3b]$$

where, t is time (s), t_s is the time at the end of the retardation period (s), G and η are the elasticity and viscosity coefficients shown in the Burger model (3a when $t < t_s$; 3b when $t \geqslant t_s$). Note that the instantaneous elastic response (at $t = 0$) and recovery (at $t = t_s$) are governed by the isolated spring G_1. The unrecoverable strain, measured as $t \to \infty$, is governed by the isolated dashpot η_1.

In addition to the 4-element Burger model the data were also fitted to several modified Burger models that included 2 and 4 element Kelvin chains. For each data set, an error in the model's ability to predict

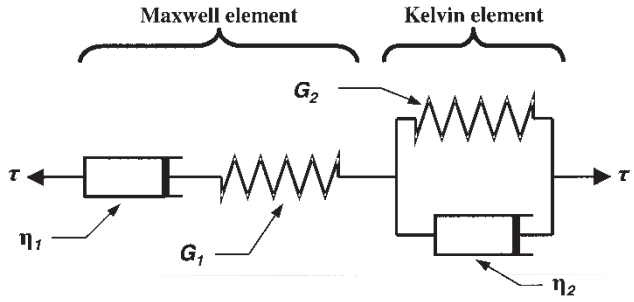

FIGURE 5 Mechanical analogue of the linear viscoelastic Burger model. G_1 and G_2 are the elastic elements (springs) and η_1 and η_2 are the viscous elements (dashpots). G_1 corresponds to I_γ (regions a and c in the creep curve shown in Figure 3), and η_1 determines V_γ (region d).

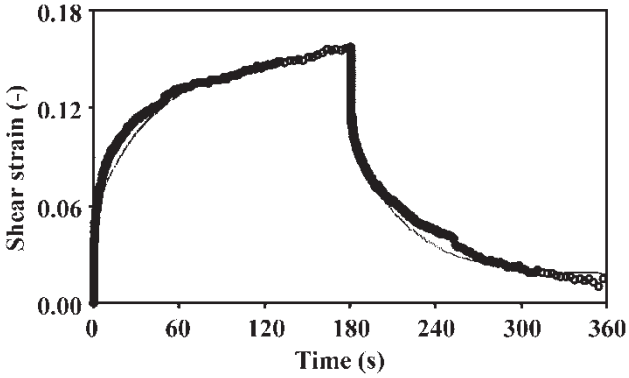

FIGURE 6 Creep data from sample 5 (circles) and the fitted data from the Burger model (line).

TABLE I Optimization results for the elastic (G) and viscous (η) elements in the Burger model fitted to data from 7 biofilm samples tested at $\tau = 0.1$ Pa. The estimates of error non-dimensional weighted optimization residual (NWR) and weighted optimization residual (WR) are also shown

Sample	1	2	3	4	5	6	7	Mean $\pm$ 1SD
G_1 (Pa)	1.94	2.53	24.20	0.30	1.19	0.81	6.78	10.8 ± 15.9
η_1 (Pa s^{-1})	27.60	148.97	380.00	10.53	45.00	36.57	404.57	477 ± 910
G_2 (Pa)	1.12	1.23	12.28	0.21	1.80	0.45	2.11	3.6 ± 4.4
η_2 (Pa s^{-1})	148.41	1100.01	4493.17	28.22	1022.22	123.14	450.41	1971 ± 2469
WR ($-$)	0.0079	0.0026	0.0003	0.0351	0.0039	0.0116	0.0032	$8.87 \pm 11.34 \times 10^{-3}$
NWR ($-$)	0.034	0.019	0.021	0.027	0.025	0.026	0.036	0.023 ± 0.007

observed strain at each time step was calculated (Table I). The maximum observed error for each time-strain series was reported by the maximum product of the residual and its time step for each data set. The mean NWR for all optimizations was approximately 2.5% and never exceeded 3.6% for any of the 8 data sets. The use of the additional Kelvin chains with the Burger model reduced the weighted residuals by no more than 4.6% for any sample. While the inclusion of these elements reduced the WR slightly, the improvements did not warrant the increased complexity of the constitutive models. Therefore, all creep curves were approximated with the 4-element Burger model (Figure 6). The resulting elastic and viscous constants are shown in Table I.

DISCUSSION

The time-dependent strain response evident in the creep curves clearly indicated that the mixed culture biofilms exhibited viscoelastic behaviour using conventional testing methods. Additionally, the capacity for unlimited deformation under a finite stress (demonstrated by the unrecoverable viscous loss) supports the classifications of these biofilms as viscoelastic fluids. The findings support conclusions drawn by previous investigators (Ohashi & Harada, 1994; Stoodley *et al*., 1999a, 2001; Korstgens *et al*., 2001) that were made through indirect or non-conventional testing. Biofilm viscoelasticity reported in these studies in pure cultures (*Pseudomonas aeruginosa* and *Delsulfovibrio* spp.), defined mixed species (*P. aeruginosa*, *K. pneumoniae*, *S. maltophilia*, and *P. fluorescens*), and engineered non-defined mixed cultures (wastewater treatment biofilms) coupled with the findings presented here for a biofilm developed from a natural surface water inoculum and from unpublished rheometry data from the authors' laboratory group on the human pathogens *Streptococcus mutans* (M Winston and P Stoodley) and *Staphylococcus aureus* (C Rupp and P Stoodley) suggest that viscoelasticity may be a general mechanical property of biofilms, despite the wide diversity in the chemistry of the extracellular polymeric substance (EPS) slime matrix (Sutherland, 2001; Allison, 2003). Since the most extensive biofilms are generally found in aqueous environments under a wide (and often fluctuating) range of fluid shears, the authors hypothesize that biofilm viscoelasticity is an adaptation for survival in moving fluids. The flow of biofilms across surfaces in response to shear forces (Stoodley *et al*., 1999b; Kolari *et al*., 2002) which may dissipate fluid energy, allowing biofilms to remain attached (Klapper *et al*., 2002), may also be responsible for the high pressure drops attributed to biofilms (Picaloglou *et al*., 1980).

However, despite the consistent viscoelastic character of the strain response, there was significant variability in the magnitudes of the elastic and viscous constants. The shear modulus (G_1) ranged over two orders of magnitude from 0.3–45 Pa and

the viscous coefficients over three orders from 10–7000 Pa.s (Table I). However, it is likely that G_1 (corresponding to I_γ) may have been overestimated by rheometer testing. In a number of the creep curves the initial elastic elongation when the shear stress was applied (a, in Figure 3) was approximately 10% larger than the elastic recoil when the stress was removed (c, in Figure 3). For a linear viscoelastic material these would be expected to be the same. One explanation is that during the initial application of shear stress there was some reconfiguring (bending in the shear direction) of biofilm structures in addition to the bulk elastic response.

The variability is not necessarily surprising given the inherent variability in density and structures reported in the biofilm literature. In future experiments characterization of the physical properties of the biofilm such as density and porosity would be useful in helping to explain the variability in mechanical properties. Another potential source of variability are differences in the surface contact between the biofilm and the rheometer base plate. However, at the gap thickness of 30 μm there was no evidence of slippage in the creep curves (which would appear as sharp downward jumps in the strain) tested at 0.1 and 0.5 Pa indicating that the surface contact was adequate for testing. In future tests such variability may be reduced by initiating the tests at a specified normal force. This would allow the gap thickness to vary with the thickness of the biofilm and the degree of surface contact with the rheometer plate. Nevertheless, a similar range of shear moduli (0.9–100 Pa) were reported for biofilms grown at varying shears by conducting stress-strain testing in flow cells (Klapper *et al.*, 2002). The similarity between shear creep curves derived from the two independent methods of rheometry (which applies and measures shear stress and strain precisely over the whole biofilm) and the flow cell method (which measures strain on the microscopic scale of individual biofilm structures but from which the stresses can only be crudely estimated) (Stoodley *et al.*, 1999a, 2002) corroborate the data from both methods.

The close agreement between the stress-strain ratio at τ = 0.1 Pa and 0.5 Pa suggested that at τ = 0.1 Pa the biofilms were in the linear viscoelastic region (*i.e.* the test itself was not changing the mechanical properties of the biofilms) and justified the use of a linear viscoelastic model for this mixed culture biofilm under these conditions. The apparent failure of the biofilm at τ of 1 Pa during methods development suggests that the yield stress of the biofilm occurred between 0.5 and 1 Pa. The use of rheometry to determine the yield point and ultimate strength of industrially and medically relevant biofilms will be useful for predicting if and when a biofilm may detach when subject to varying shear.

Significance of the Linear Biofilm Model

The results have demonstrated that the biofilm strain response to shear stress combines viscous and elastic behaviour in a linear fashion that can be approximated by a 4-element linear viscoelastic Burger model. It is important to note that the Burger model was applicable despite the wide range in strain responses though individual parameters varied widely from sample to sample. This is the first step in the development a comprehensive constitutive model for biofilms. Although the model is only applicable in the linear region, below the yield point, and therefore cannot currently be used to predict failure, future work will include coupling this model with hydrodynamic and failure models. Incorporating this material response, as a compliant boundary condition, with hydrodynamic models would permit the analysis and design of biofilm-influenced flow. Such a model may permit the engineer to predict pressure drops caused by biofilm growth in piping networks and the skin drag on ship hulls. Furthermore, by augmenting this study with measurements of biofilm failure at varying stress levels in the rheometer and direct observation of shear induced detachment in flow cells (Stoodley *et al.*, 2002), it may be possible to incorporate failure levels into this linear model. The applications of this technology would include designing the flow dynamics of artificial heart implants and water distribution systems in order to minimize contamination caused by fluid-induced biofilm detachment.

Nomenclature

Dimensions in terms of mass (M), length (L) and time (T)

c	linear proportionality constant (*dimensionless*)
C_S	maximum observed creep modulus ($M/L{\cdot}T^2$)
G	elastic modulus ($M/L{\cdot}T^2$)
γ	shear strain (M/M)
γ_O	observed shear strain (M/M)
γ_P	predicted shear strain (M/M)
η	viscosity coefficients ($M/L{\cdot}T$)
I_γ	instantaneous elastic strain response (M/M)
NWR	non-dimensional weighted optimization residual (*dimensionless*)
R^2	regression correlation coefficient (*dimensionless*)
R_I	ratio of unrecoverable viscous strain to maximum strain (*dimensionless*)
R_V	ratio of instantaneous elastic strain to maximum strain (*dimensionless*)
τ	shear stress ($M/L{\cdot}T^2$)
θ_H	hydraulic residence time (T)
t_s	time of transition from retardation to creep recovery (T)
V_γ	unrecoverable viscous strain (M/M)
WR	weighted optimization residual (M/M)

Acknowledgements

This work was funded by the National Institutes of Health RO1 grant GM60052-02 and in part by the co-operative agreement EEC-8907039 between the National Science Foundation and Montana State University, Bozeman and the W M Keck Foundation. For their technical advice and contributions we thank Ladean McKittrick, Department of Civil Engineering, Alexandra Vinogradov, Department of Mechanical Engineering, Isaac Klapper, Department of Mathematics and Ryan Cargo, the Center for Biofilm Engineering at Montana State University, Bozeman, Montana.

References

Allison D G (2003) The biofilm matrix. *Biofouling* **19**: 139–150

Characklis W G (1973) Attached microbial growth. II Frictional resistance due to microbial slimes. *Water Res* **7**: 1249–1258

Cooksey K E, Wigglesworth-Cooksey B (1995) Adhesion of bacteria and diatoms to surfaces in the sea: a review. *Aquat Microb Ecol* **9**: 87–96

Costerton J W, Stewart P S, Greenberg E P (1999) Bacterial biofilms: a common cause of persistent infections. *Science* **284**: 1318–1322

Findley W N, Lai J S, Onaran K (1989) *Creep and Relaxation of Nonlinear Viscoelastic Materials*. Dover Publishing, Minneola, NY

Flemming H-C, Wingender J, Mayer C, Koerstgens V, Borchard W (2000) Cohesiveness in biofilm matrix polymers. In: Allison D, Gilbert P, Lappin-Scott H M, Wilson M (eds) *Community Structure and Cooperation in Biofilms.* SGM Symposium Series 59, Cambridge University Press, Cambridge, pp 87–105

Flugge W F (1975) *Viscoelasticity*, 2nd Edition. Springer-Verlag, New York, NY

Klapper I, Rupp C J, Cargo R, Purevdorj B, Stoodley P (2002) A viscoelastic fluid description of bacterial biofilm material properties. *Biotech Bioeng* **80**: 289–296

Kolari M, Schmidt U, Kuismanen E, Salkinoja-Salonen M S (2002) Firm but slippery attachment of *Deinococcus geothermalis*. *J Bacteriol* **184**: 2473–2480

Koerstgens V, Flemming H-C, Wingender J, Borchard W (2001) Influence of calcium ions on the mechanical properties of a model biofilm of mucoid *Pseudomonas aeruginosa*. *Water Sci Technol* **43**: 49–57

Mase G T, Mase G E (1999) *Continuum Mechanics for Engineers*, 2nd Edition. CRC Press LLC, Boca Raton, FL

Newman H N (1998) Periodontal therapeutics – a viable option? *Int Dent J* **48**: 173–179

Ohashi A, Harada H (1994) Adhesion strength of biofilm developed in an attached-growth reactor. *Water Sci Technol* **29**: 281–288

Picologlou B F, Zelver N, Characklis W G (1980) Biofilm growth and hydraulic performance. *J Hydraul Div Am Soc Civ Eng* **106**(No HY5): 733–746

Schultz M, Swain G W (2000) The influence of biofilms on skin friction drag. *Biofouling* **15**: 129–139

Stoodley P, Lewandowski Z, Boyle J D, Lappin-Scott H M (1999a) Structural deformation of bacterial biofilms caused by short term fluctuations in flow velocity: an *in situ* demonstration of biofilm viscoelasticity. *Biotech Bioeng* **65**: 83–92

Stoodley P, Lewandowski Z, Boyle J D, Lappin-Scott H M (1999b) The formation of migratory ripples in a mixed species bacterial biofilm growing in turbulent flow. *Environ Microbiol* **1**: 447–457

Stoodley P, Cargo R, Rupp C J, Wilson S, Klapper I (2002) Biofilm mechanics and shear induced deformation and detachment. *J Ind Microbiol Biotech* **29**: 361–368

Stoodley P, Jacobsen A, Dunsmore B C, Purevdorj B, Wilson S, Lappin-Scott H M, Costerton J W (2001) The influence of fluid shear and $AlCl_3$ on the material properties of *Pseudomonas aeruginosa* PAO1 and *Desulfovibrio* sp. EX265 biofilms. *Water Sci Technol* **43**: 113–120

Sutherland I W (2001) The biofilm matrix: an immobilized but dynamic microbial environment. *Trends Microbiol* **9**: 222–227

Townsin R L (2003) The ship hull fouling penalty. *Biofouling* **19**(Suppl): 9–15

Walker J T, Mackerness C W, Mallon D, Makin T, Williets T, Keevil C W (1995) Control of *Legionella pneumophila* in a hospital water-system by chlorine dioxide. *J Ind Microbiol* **15**: 384–390

Zelver N (1979) Biofilm development and associated energy losses in water conduits. MS Thesis, Rice University, Houston, TX